

SUPPLEMENTARY INFORMATION
for Langowski *et al.*,
Nature Manuscript #2005-06-07073C

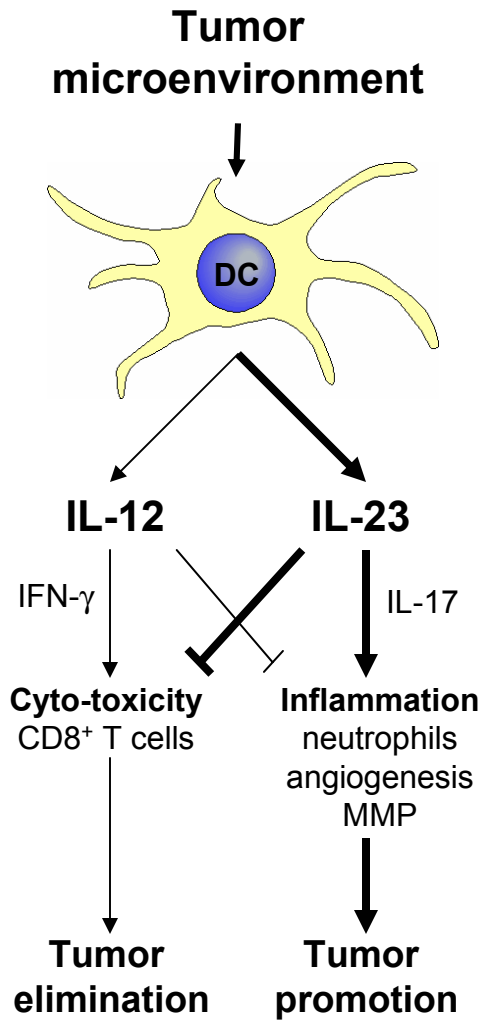


Figure S1 | Proposed mechanism of tumor promotion by deregulation of the IL-12 / IL-23 family of cytokines.

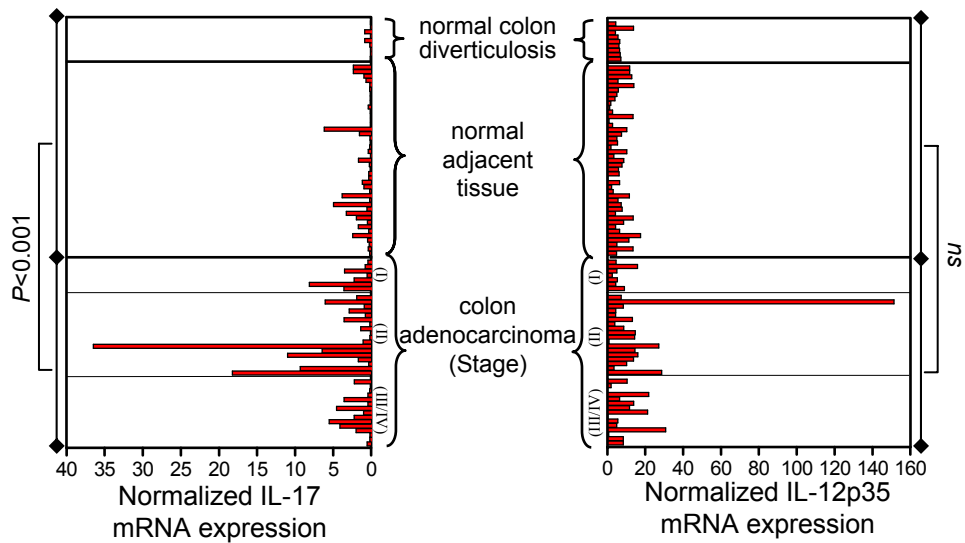
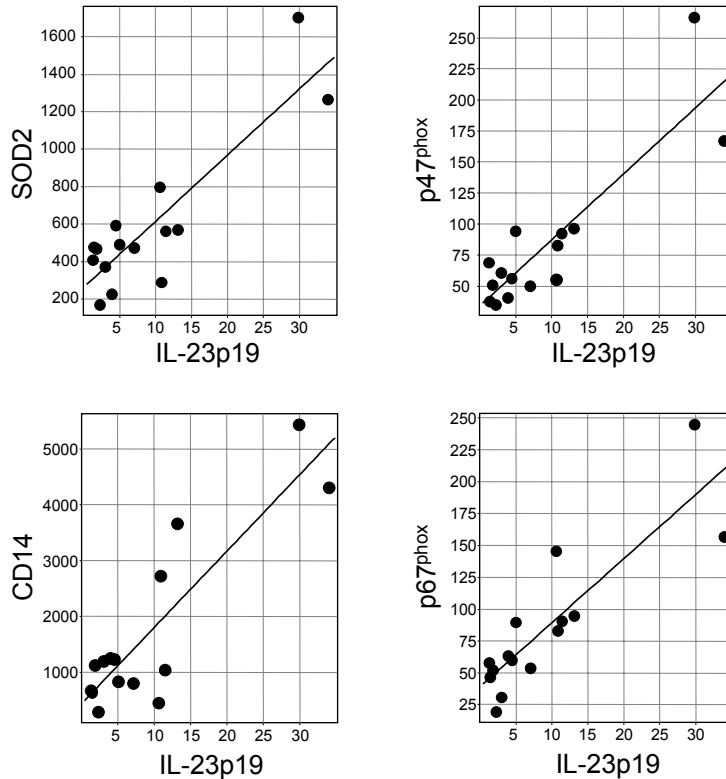


Figure S2 | Increased IL-17 but not IL-12p35 expression in human colon adenocarcinoma. Quantitative mRNA expression; each y-axis position signifies an individual patient sample with expression of p19 and p40. Histological classification of samples as normal, normal adjacent and cancerous (with stage classification) is given.

a**b**

Gene	R ²	IL-23p19 correlation (P)
SOD2	0.77	1.83E-05
p47 ^{phox}	0.77	1.85E-05
CD14	0.77	2.23E-05
p67 ^{phox}	0.75	2.96E-05

Figure S3 | Correlation of cellular markers with IL-23p19 expression within human colorectal tumors. a-b, Linear regression analysis of stage III and IV colon carcinoma shows significant correlation between the expression of IL-23p19 with markers for the myelomonocytic lineage (CD14) and neutrophil activation states (superoxide dismutase 2 – SOD2, p47^{phox}, p67^{phox}); significance of correlation is expressed by R² and P (n=16).

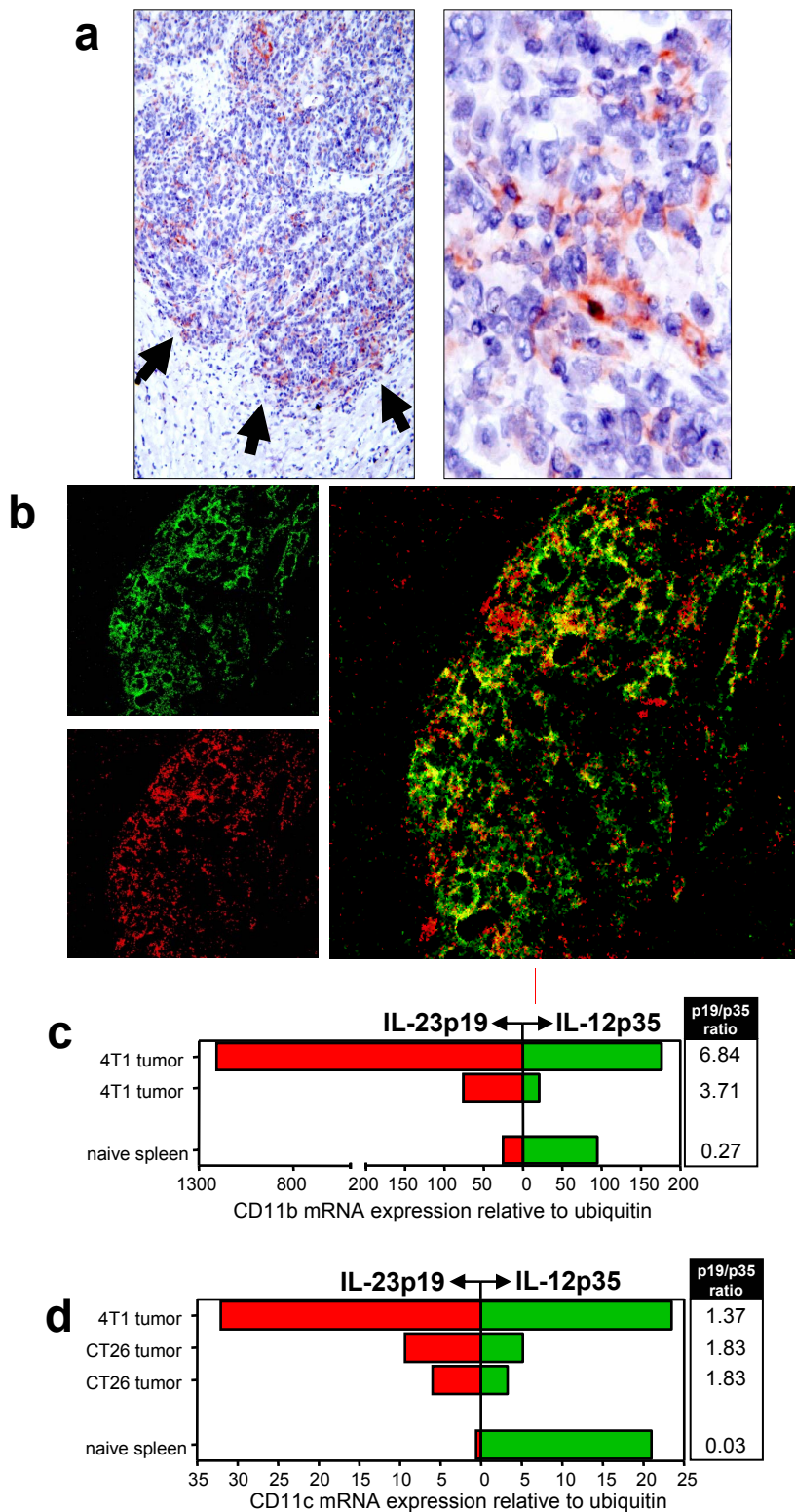


Figure S4 | IL-23p19 expression within human and mouse tumors. **a**, Immunohistochemistry of human ovarian carcinoma showing IL-23p19 expression (red) within human ovarian carcinoma (arrowheads) but not in the adjacent stroma. **b**, Confocal fluorescent microscopy of human ovarian carcinoma utilizing antibodies against IL-23p19 (red) and the dendritic cell marker CD11c (green) shows IL-23 expression localized and overlapping (yellow) with CD11c infiltration. Murine CD11b (**c**) and CD11c (**d**) cells isolated from subcutaneous 4T1 breast or CT26 colon tumor masses exhibit greatly potentiated IL-23p19 mRNA expression when compared naïve splenic counterparts. IL-12p35 expression is relatively unchanged. The table depicts the ratio of p19 to p35 mRNA expression.

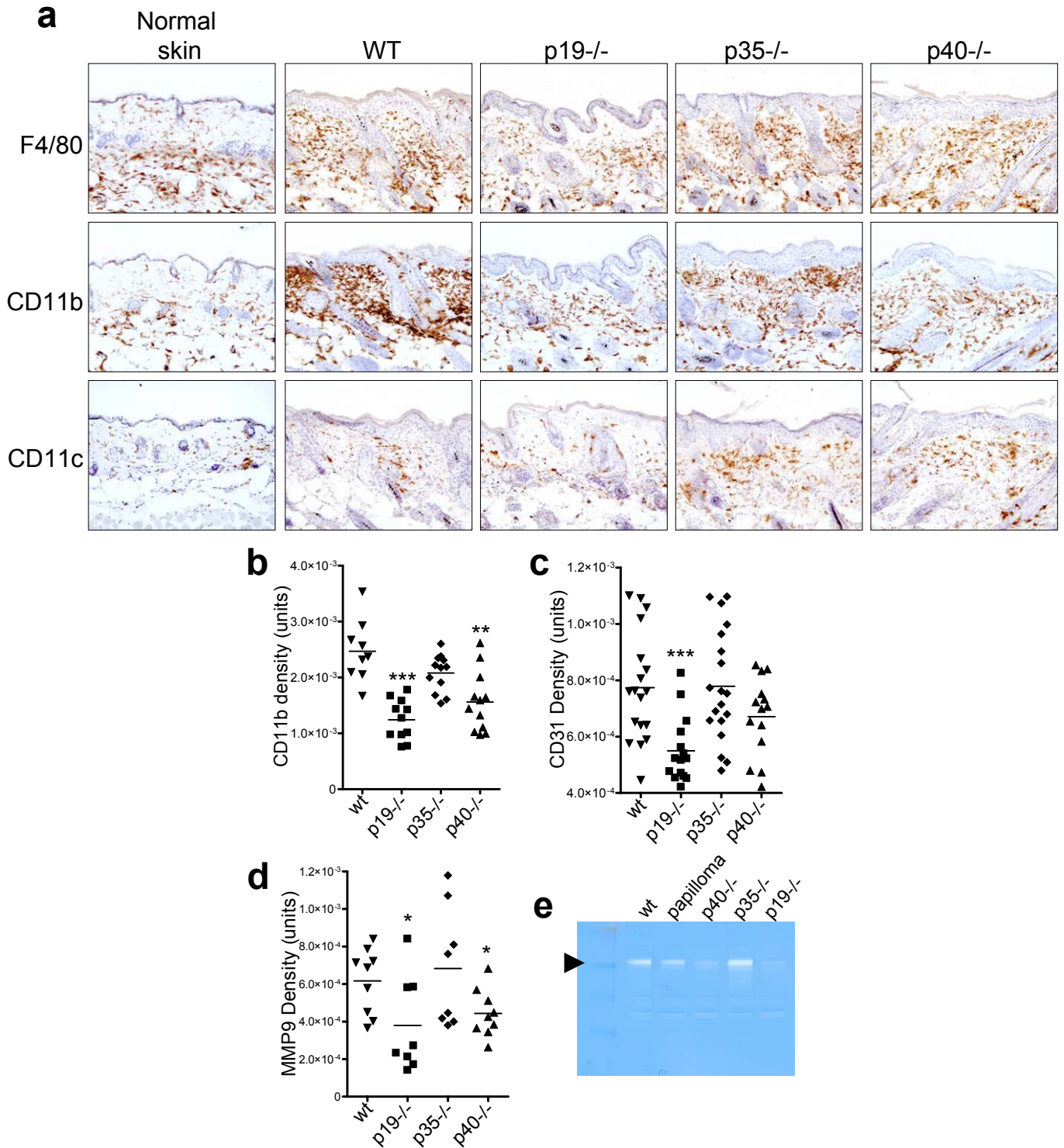


Figure S5 | Inflammatory cell markers and mediators in carcinogen-treated skin. **a**, Presence of F4/80, CD11b and CD11c-positive cells within carcinogen-treated murine skin compared to normal naïve skin. **b-d**, Densitometric analysis of immunohistochemistry following 140 days of carcinogenesis. Mice lacking IL-23p19 exhibit greater CD11b staining (**b**), vessel density (**c**) and increased MMP9 expression (**d**). **e**, Zymogram of carcinogen-treated skin shows increased enzymatic activity of MMP9 in wt and IL12p35^{-/-} mice but not IL-23 deficient animals. Data are mean \pm s.d.; scatter plots show staining density with bars depicting the mean. Significance of results in figures is represented by * ($P < 0.05$), ** ($P < 0.01$) and *** ($P < 0.001$).

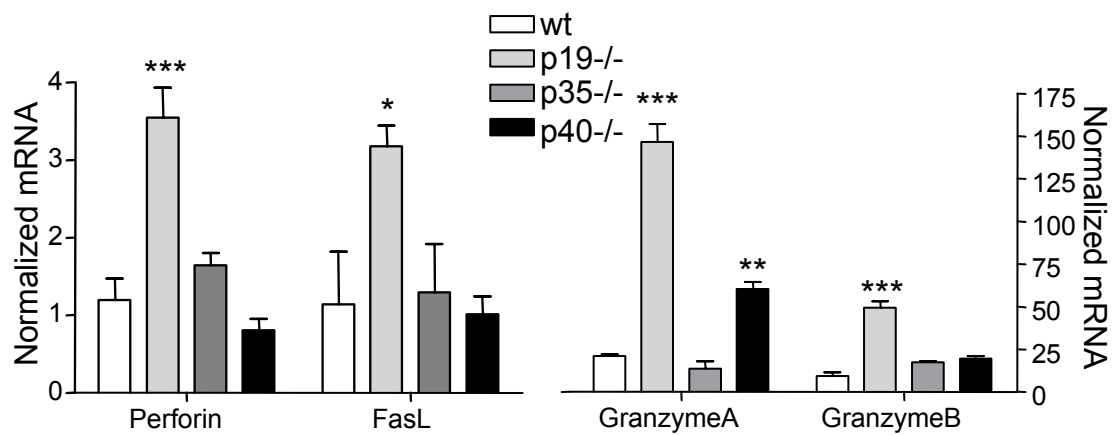


Figure S6 | Cytotoxic cell markers in carcinogen-treated skin. Expression of markers for cytotoxicity are elevated in IL-23p19 deficient mice. Significance of results in figures is represented by * ($P < 0.05$), ** ($P < 0.01$) and *** ($P < 0.001$).

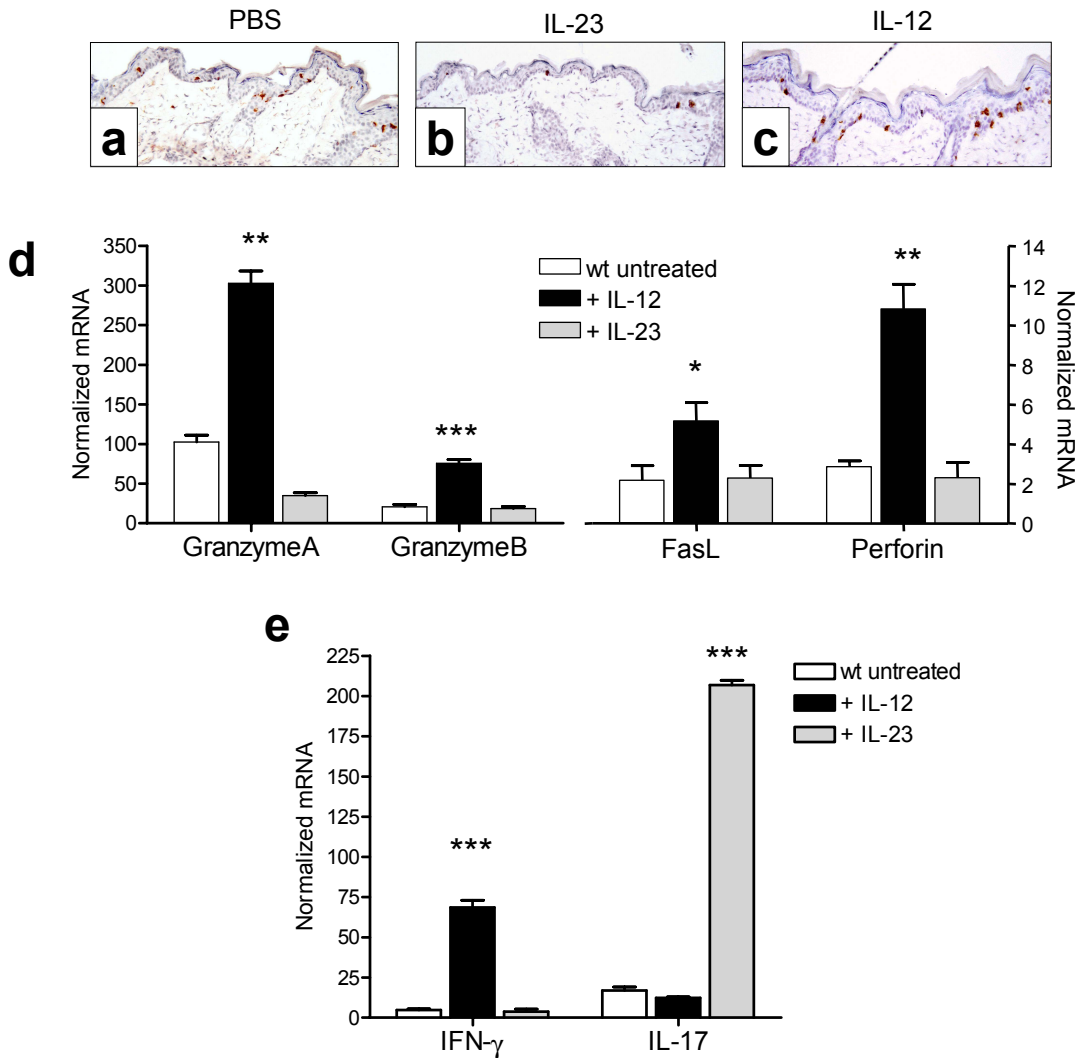


Figure S7 | IL-12 stimulates, but IL-23 decreases immune surveillance by CD8 T-cells. **a-c**, Epithelial CD8 infiltration following treatment with exogenous IL-23 (**b**) or IL-12 (**c**) compared to control treated animals (**a**). **d-e**, Cytokine and cytotoxic marker mRNA expression in carcinogen treated skins in response to IL-12, IL-23 or PBS treatment. IL-12 administration increases perforin, granzyme, FasL and IFN- γ (**d**), while IL-23 administration potentiates IL-17 expression (**e**). Significance of results in figures is represented by * ($P < 0.05$), ** ($P < 0.01$) and *** ($P < 0.001$).

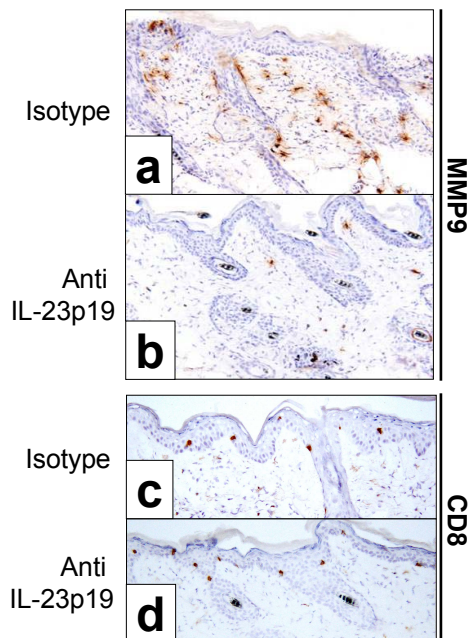


Figure S8 | IL-23 ablation decreases inflammatory markers, increases immune surveillance. Systemic treatment with anti-IL-23p19 antibody shows marked decrease in MMP9 expression (**b**), but increase in CD8+ T-cells (**d**) compared to control.

Supplementary Methods

Animals

IL-23p19^{-/-} were produced by DNAX with congenic N7 offspring on the C57BL/6 background created in concert with The Jackson Laboratory utilizing a speed-congenic method and SSLP markers for screening. IL-23R^{-/-} mice were generated at Xenogen Biosciences. Utilizing the mL-23R sequence a database search identified a BAC clone containing the IL-23R locus. The targeting vector was constructed with a 5' homologous arm (3.2kb) and 3' homologous arm (4.4kb) using PCR. The targeted locus has exons 1-3 replaced with an FRT flanked Neo cassette. The targeting vector was electroporated into C57BL/6 ES cells and G418 resistant colonies were screened for homologous recombination by Southern blotting with a probe flanking the 3' arm. IL-23R^{-/-} and wild-type controls were maintained on a C57BL/6 background.

Human tissue samples

All human tissues were obtained under IRB approved protocols. Depending on the collection protocols established at each site, tissues were acquired either under IRB-approved waiver of consent (NDRI and CHTN) or by informed consent (PAH, Zoion, Ardais, and AGF). All samples have been de-identified or anonymized, so investigators have no ability to identify the patients. Paired human tumor and normal adjacent tissues were obtained from patients undergoing routine therapeutic surgery from the following sources: Dr. David Gotley of the Princess Alexandra Tumour Tissue Bank (PAH) in Woolloongabba, Queensland Australia, Zoion Diagnostics, Hawthorne, New York, and National Disease Research Interchange (NDRI), Philadelphia, PA. Normal human tissue were obtained from patients undergoing routine surgery (multiple tissue - NDRI; Stomach - Ardais Corporation, Lexington, MA, and Colon - Cooperative Human Tissue Network (CHTN), Nashville, TN), from short hour autopsy (≤ 5 hours, multiple tissues - Zoion Diagnostics), and from transplant donors (Lung - Anatomical Gift Foundation, Hanover, MD). All surgical samples were frozen as quickly as possible, typically within an hour of excision. The majority of samples were accompanied by demographic information and pathology reports.

Gene Expression Analysis

For TAQMAN analysis, total RNA was isolated using RNA STAT-60 (Tel-Test, Friendswood, TX, USA) according to manufacturer's instructions. After isopropanol precipitation, total RNA was re-extracted with phenol:chloroform:isoamyl alcohol (25:24:1; Sigma Chemicals) using phase-lock light tubes (Eppendorf). Total RNA (5 μ g) was subjected to treatment with DNase (Roche) according to manufacturer's instructions. RNA integrity was verified by gel electrophoresis, and only samples with intact ribosomal RNA bands were included. DNase-treated total RNA was reverse-transcribed using Superscript II (Gibco/BRL) according to manufacturer's instructions. Further analysis was performed firstly on pools of samples with identical conditions, followed by single sample analysis for statistical analysis. Primers were designed using Primer Express (PE Biosystems), or obtained commercially from Applied Biosystems. Real-time quantitative PCR on 10 ng of cDNA from each sample was performed using either of two methods. In the first method, two gene-specific unlabelled primers were utilized at 400 nM in a Perkin Elmer SYBR green real-time quantitative PCR assay utilizing an ABI 5700 instrument. In the second method, two unlabelled primers at 900 nM each were used with 250 nM of FAM-labelled probe (Applied Biosystems) in a TAQMANTM real-time quantitative PCR reaction on an ABI 7700 sequence detection system. The absence of genomic DNA contamination was confirmed using primers that recognize genomic region of the CD4 promoter - samples with detectable DNA contamination by real-time PCR were excluded from the study. Ubiquitin levels were measured in a separate reaction and used to normalize the data by the $\Delta - \Delta$ Ct method, using the mean cycle threshold (Ct) value for ubiquitin and the gene of interests for each sample; the equation $1.8^e (Ct \text{ ubiquitin} - Ct \text{ gene of interest}) \times 10^4$ was used to obtain the normalized values. For murine samples, punch biopsies were taken from at least three independent, macroscopically and histological tumor free areas for each condition.